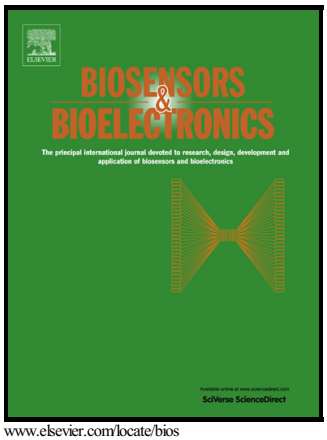

www.elsevier.com/locate/bios

Colorimetric monitoring of rolling circle amplification for detection of H_5N_1 influenza virus using metal indicator

Seyed Vahid Hamidi, Hedayatollah Ghourchian

PII: S0956-5663(15)30079-8
DOI: http://dx.doi.org/10.1016/j.bios.2015.04.078
Reference: BIOS7646

To appear in: *Biosensors and Bioelectronic*

Received date: 9 March 2015
Revised date: 22 April 2015
Accepted date: 23 April 2015

Cite this article as: Seyed Vahid Hamidi and Hedayatollah Ghourchian, Colorimetric monitoring of rolling circle amplification for detection of H_5N_1 influenza virus using metal indicator, *Biosensors and Bioelectronic,* http://dx.doi.org/10.1016/j.bios.2015.04.078

Colorimetric monitoring of rolling circle amplification for detection of H_5N_1 influenza virus using metal indicator

Seyed Vahid Hamidi, Hedayatollah Ghourchian*

Laboratory of Microanalysis, Institute of Biochemistry and Biophysics, University of Tehran, P.O. Box 131451384, Tehran, Iran

Nanobiomedicine Center of Excellence, Nanoscience and Nanotechnology Research Center, University of Tehran, P.O. Box 131451384, Tehran, Iran

To whom correspondence should be addressed.

* Corresponding author. Tel.: +98 21 66408920, Fax: +98 21 66404680
E-mail addresses: ghourchian@ut.ac.ir

Abstract

A new colorimetric method for monitoring of rolling circle amplification was developed. At first H_5N_1 target hybrids with padlock probe (PLP) and then PLP is circularized upon the action of T_4 ligase enzyme. Subsequently, the circular probe is served as a template for hyperbranched rolling circle amplification (HRCA) by utilizing Bst DNA polymerase enzyme. By improving the reaction, pyrophosphate is produced via DNA polymerization and chelates the Mg^{2+} in the buffer solution. This causes change in solution color in the presence of hydroxy naphthol blue (HNB) as a metal indicator. By using pH shock instead of heat shock and isothermal RCA reaction not only the procedure becomes easier, but also application of HNB for colorimetric detection of RCA reaction further simplifies the assay. The responses of the biosensor toward H_5N_1 were

linear in the concentration range from 0.16 to 1.20 picomolar with a detection limit of 28 femtomolar.

Keywords: Rolling circle amplification, H_5N_1 virus, Bst DNA polymerase, Hydroxy naphthol blue, pH shock

1. Introduction

One of the most leading causes of worldwide and specially childhood disease is acute respiratory infections (Quan et al. 2007; Williams et al. 2002). It is reported that it caused 1.9 million deaths in 2000 of which 1 to 3% and 10 to 25% of them had less than 5 years of age in industrialized and developing countries, respectively (Nijhuis et al. 2002). Outbreaks of influenza viruses in both human and animals lead to considerable economical impacts such as medical cure, loss of working times and animal stocks as well (Gyarmati et al. 2008). It is estimated that only influenza virus, annually costs for about $ 10.4 billion in United States (Molinari et al. 2007). Based on the structural genes, influenza viruses are divided into A, B and C types. Among them type A viruses encompass wide spectrum of hosts and also are more virulent (Gyarmati et al. 2008). Influenza A viruses are categorized according to two surface antigens which are called hemagglutinin (HA) and neuraminidase (Wang et al. 2002). The genome of type A contains 8 RNA segments which changes overtime due to mechanisms of antigenic shift and antigenic drift (Webster et al. 1992). However, antigenic drift results in major changes because it introduces antigenically novel influenza A viruses in to population. The global outbreak of bird flu or avian influenza A (subtype H_5N_1) in 2003 had such a huge

worldwide impacts that attracted attentions toward H_5N_1 virus (Li et al. 2004). Bird flu is known that it is highly pathogenic in aquatic birds, but human infections have been reported leading to death (Dawson et al. 2007). Thus, influenza A viruses and specially H_5N_1 subtype have caused a great public and scientific concern (Stöhr 2003).

Rolling circle amplification (RCA) is a bio-mimetic isothermal amplification technique and because of robustness and simplicity has a special position among other isothermal amplification techniques (Demidov 2002). Hyperbranched rolling circle amplification (HRCA) is one of the modes of the RCA reaction in which more than one primer (a strand of nucleic acid that serves as a starting point for DNA synthesis in RCA reaction initiation and ramification) is undergone, so that the signal will be much more amplified (Hamidi et al. 2015). For the first time, RCA has been used to enhance restriction enzyme analysis, cloning and sequencing, for the purpose of detecting novel variants of circular DNA viruses such as papilloma viruses subtypes (Rector et al. 2004). However, in order to detect viruses with linear DNA, it is necessary to provide circular template which is the fundamental basic of RCA reaction. Padlock probes (PLPs) was first introduced for the detection of linear targets by Nilsson et al (Nilsson et al. 1994). PLP is circularizable probe that consisting of two specific sequences to detect the target and also a linker region to help formation of circular template and provide space for hybridization of RCA primers (Hamidi et al. 2015).

So far, turbidity test is used to determine a positive loop-mediated isothermal amplification (LAMP) reaction (Goto et al. 2009). Because during a LAMP reaction pyrophosphate (PPi^-) is produced as a byproduct which causes the reaction solution turns unclear after chelating with Mg^{2+} (Mori et al. 2001). Thus, monitoring of the reaction solution with a real-time turbidimeter has been widely used for quantifying DNA samples (Mori et al. 2004; Thai et al. 2004;

Yoneyama et al. 2007). Hydroxy naphthol blue (HNB) was previously used for determination of total water hardness including magnesium and calcium ions in water (Brittain 1977; Nakajima et al. 2003). In 2009, for the first time HNB was utilized for colorimetric detection of LAMP products via Mg^{2+} concentration change (Goto et al. 2009). Thereafter, HNB was widely used for detection of different targets including influenza A viruses subtypes by using LAMP technique (Ma et al. 2010; Nie et al. 2013; Zhang et al. 2013). However, in the present study HNB was first employed for colorimetric determination of RCA products.

So far heat shock was used for denaturation of DNA samples. In fact denaturation of DNA at high temperature (95 °C) leads to possible breaks in DNA strands and also it demands a device for increasing the temperature. Therefore, in the present study the heat shock was replaced by pH shock due to the following advantages: i) by excluding the need for thermal device the procedure became much simpler. ii) replacement of heat shock by pH shock protects DNA from possible breaks which occurs at high temperature (Hamidi et al. 2015). In addition, in the present work HNB has been first applied for colorimetric detection of RCA reaction when coupled with large fragment of Bst DNA polymerase. Bst DNA polymerase is high efficient for HRCA reaction (Lizardi et al. 1998; Zhang et al. 2001a) that allow us to achieve fine sensitivity and low detection limit for H_5N_1 assay.

2. **Materials and methods**

2.1. Oligonucleotides

The forward and reverse primers, PLP (5` phosphorylated) and synthetic target were the same sequences as that were used in our previous study (Hamidi et al. 2015). The recognition site for PLP was chosen from the most conserved part of H_5N_1 HA gene and was evaluated by

basic local alignment search tool (BLAST) program (http://blast.ncbi.nlm.nih.gov) (Gyarmati et al. 2008; Hamidi et al. 2015; Wang et al. 2005). The selected sequence was 100 percent conserved among all H_5N_1 genomes that were reported in genome database. The primers, probe and synthetic target were obtained from Metabion (Germany) (Hamidi et al. 2015).

2.2 cDNA preparation

The positive H_5N_1 bird's samples were obtained from Tehran University of Medical Sciences in which the concentrations were determined by using conventional real-time PCR device. RNA extraction was performed by utilizing RNA extraction kit (Jena Bioscience, Germany) and thereafter, complementary DNA (cDNA) was produced by RevertAid First Strand cDNA Synthesis Kit (Fermentas, USA). In this procedure temperature was regulated in thermo cycler (Thermo, Express, UK).

2.3.Colorimetric determination of H_5N_1

2.3.1. pH shock for PLP ligation: In order to denature DNA, 1 µl of PLP and 1 µl of sample cDNA were added to 1.2 µl of denaturing solution (10 mM EDTA and 400 mM KOH, pH: 12). Thereafter, the solution was uniformed via pipetting the mixture which follows by incubating for 3 min at room temperature. After that, 0.8 µl of neutralizing solution (600 mM Tris-HCl and 400 mM HCl) was slowly added to the solution in order to neutralize the reaction mixture and make it possible for PLP to hybridize with the H_5N_1 target (Hamidi et al. 2015). In the next step, 1 µl of the ligation mixture including 0.5 µl of 10X T_4 ligase buffer (400 mM Tris-HCl, pH 7.9, 100 mM $MgCl_2$, 100 mM DTT, 5 mM ATP) and 0.5 µl deionized water was poured into the reaction mixture. The ligation reaction has been carried out by adding of 2 units (U) of T_4 ligase enzyme

to the reaction via incubation at 37 °C for 60 min (Wang et al. 2014). At the end, the enzyme was inactivated by increasing up the temperature to 70 °C for 5 min.

2.3.2. Exonucleolysis: In the next step, in order to exclude the unligated PLP and also make it possible for the amplification enzyme to perform RCA reaction, exonucleolysis step has been done (Banér et al. 1998). The exonuclease treatment was carried out by injecting 1 µl of 10X NEBuffer 1 and 10 U of exonucleases I (New England Biolabs, Ipswich, MA) into the ligation mixture in the final volume of 10 µl and incubating at 37 °C for 30 min. The exonucleolysis reaction was terminated by heating 80 °C for 20 min.

2.3.3. HRCA reaction: The HRCA reaction was carried out in the final volume of 25 µl by injecting 10 µl exonucleolysis mixture to the solution containing 10X Bst DNA polymerase enzyme buffer containing 400 mM Tris-HCl (pH 8.8), 200 mM KCl, 160 mM $MgSO_4$, 200 mM $(NH_4)_2SO_4$, Tween 0.2 % (which all obtained from Merck, USA) and 16 M Betaine (Sigma-Aldrich, USA) (Goto et al. 2009; Tomita et al. 2008) were added to 2 mM deoxyribonucleotide triphosphate (dNTP) (Fermentas, USA), 10 picomolar (pM) forward primer, 10 pM reverse primer, 8 U of large fragment Bst DNA polymerase (Kaocharoen et al. 2008; Steain et al. 2009) (New England Biolabs, Ipswich, MA) and 120 µM hydroxyl naphthol blue (HNB) (Goto et al. 2009) (Sigma-Aldrich, USA). The HRCA reaction was performed at 63 °C for 60 min where temperature was adjusted by thermo cycler (Liang et al. 2014; Zhang et al. 2001b) (Thermo, Express, United Kingdom) and then to inactivate Bst DNA polymerase enzyme and terminate the reaction, according to the procedure recommended by the company (New England Biolabs, Ipswich, MA), the temperature was kept at 80 °C for 20 min.

2.3.4. Colorimetric measurement: Next, the mixture was transferred to plate with 384 wells (Greiner Bio-One, Germany) and then the plate was placed in micro plate reader instrument (H4, Biotek, USA). Then the absorbance intensity was recorded in spectrum of 600 to 700 nm. It is worth to mention that the overall time spent for all these procedures (illustrated in Scheme 1), was about 200 min.

2.4. Gel electrophoresis assay

Visualizing of HRCA products via gel electrophoresis was performed in 1% agarose gels which contains 0.25 gr agarose powder (Amersham Pharmacia Biotech, Sweden) and 25 ml TAE buffer containing 40 mM Tris-acetate, 1 mM EDTA, pH 8.0 (Sigma-Aldrich, USA). The electrophoresis procedure was performed under the applied voltage of 90 V for 30 min and after which the gel was placed in ethidium bromide (Sigma-Aldrich, USA) solution in order to HRCA products can be visualized by transilluminator (SynGen, United Kingdom).

2.5. Real sample assay

In order to evaluate respond of the propose biosensor in real condition, 5 positive real samples was examined where their concentration were determined by the conventional real-time PCR (Qiagen, Rotor-Gene, Germany) utilizing real-time PCR kit (Genesig, United Kingdom). Then their responds were compared with each others to determine the reality of proposed method responds.

It is worth to mention that all of the experiments in this report were performed three times and the graphs are plotted based on the mean values of experimental data.

3. Results and Discussion

3.1. HNB as an indicator for RCA monitoring

HNB has a red color at pH 4 and transition from red to blue occurs by pH change from 4 to 5, after which it remains in blue color in the pH ranges from 5 to 14. The pure red HNB solution shows a single peak at 530 nm while in blue form it represents a spectrum at 650 nm. It is worth to note that the extinction coefficient at 650 nm is higher than that at 530 nm (Brittain 1977). HNB has been reported as a metallochromic indicator for assaying of Mg^{2+} at pH about 10 (Ito and Ueno 1970). It means that in the presence of Mg^{2+}, HNB chelates the metallic ions to form HNB-Mg complex (Reaction 1). At pH 8.8, by formation of this complex the absorption intensity at 650 decreases while a new peak appears at 530 nm. On the other hand, HNB can be used for monitoring of RCA reaction via the changes in the concentration of soluble Mg^{2+}, because large fragment of Bst DNA polymerase performs DNA polymerization at pH 8.8 (Goto et al. 2009) (Reactions 2). By chelating of the soluble magnesium by PPi^{-} (Reaction 3), Reaction 1 is going in reverse direction. Therefore, the color of the solution changes from dark blue to sky blue. This color change is possible to be recognized even by naked-eye (Nahar et al. 2015; Safavieh et al. 2014). All in all, the absorption intensity of HNB at λ_{max} 650 nm has been chosen for determination of RCA due to the fact that: i) the extinction coefficient at 650 nm is higher than that at 530 nm, ii) the absorption intensity of HNB at λ_{max} 650 nm is concomitant with the Mg^{2+} concentrations (Brittain 1977; Nakajima et al. 2003).

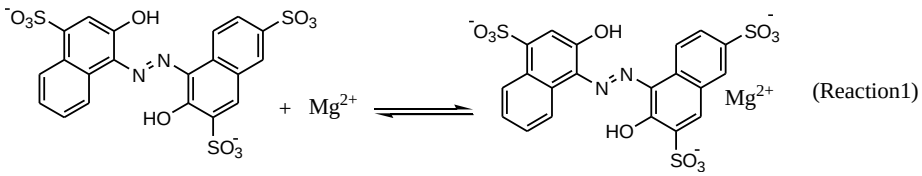

(Reaction1)

HNB, Sky blue (λ_{max} 650 nm) Dark blue (λ_{max} 530 nm)

dNTP + Bst DNA polymerase ⟶ dNMP + PPi^{-} (Reaction 2)

$PPi^{-} + Mg^{2+} \rightleftharpoons PPi\text{—}Mg$ (Reaction 3)

3.2. Monitoring of HRCA products

In HRCA reaction, signal is amplified via DNA ramification which produces double strand DNA (dsDNA) with different molecular weights. In order to monitor HRCA products, the HRCA reaction was carried out in the absence and presence of H_5N_1 target and the resulted products were separated via gel electrophoresis (Fig. 1). As seen no products were observed in the sample without H_5N_1 target (Lane A) while, in the presence of H_5N_1 target, different products were appeared in smear form which centered around 800 to 900 base pairs region (Lane B). DNA ramification happens due to strong helicase activity of large fragment Bst DNA polymerase. The products encompass wide spectrum of dsDNA, therefore, this is why DNA ramification products will be monitored like a smear in electrophoresis gel.

3.3. Optimization of analytical parameters of HRCA reaction

3.3.1. PLP concentration Since the concentration of the PLP affects on the sensitivity of RCA assay as well as on the intensity of signals, in this experiment the concentration of the PLP was first optimized. For this purpose, HRCA reaction was done at 63 ˚C and in the constant target concentration (0.40 pM) and different PLP concentrations (0, 0.2, 0.4, 0.6 and 0.8 pM) (Fig. 2A). Fig. 2A (Inset 1) concludes that an increase in PLP concentration is concomitant with increasing the intensity of signal. This also can be easily observed by naked-eyes because of the striking change in the color of solution from dark blue to sky blue (Inset 2). However, by raising the concentration up to 0.6 pM the signal reached to a plateau and as a result it was selected as optimum concentration for PLP. Another fact worth noticing is that much further rising in the

concentration of PLP causes declining the signal due to inappropriate hybridization of two PLPs with a target (Hamidi et al. 2015).

3.3.2. dNTPs concentration The other parameter that was investigated in this study was the concentration of dNTPs. The increment of dNTPs concentration has direct effect on the efficiency of polymerization reaction for the reason that it increases accessible dNTPs for large fragment of Bst DNA polymerase to perform HRCA reaction. Therefore, in this research HRCA reaction was carried out in the constant concentration of PLP (0.6 pM), target (0.40 pM) and different concentrations of dNTP (0, 0.50, 1.0, 1.50, 2.0 and 2.50 mM) at 63 ˚C (Fig. 2B). As seen in Inset 1, the absorbance intensity increased linearly up to 2.0 mM of dNTP concentration. Thus, it was chosen as an optimized concentration throughout this work. It is also noticeable that addition of dNTP to the HNB solution prior the amplification reaction is leaded to change the color of solution from magenta to dark blue (Inset 2, tube II). It has been reported that this event is induced via the chelation of Mg^{2+} by dNTPs (Goto et al. 2009).

3.3.3. Mg^{2+} concentration As a matter of fact, Mg^{2+} plays an essential role in bio-catalytic activity of DNA polymerase enzymes (Steitz 1998). Also as described earlier, the color of HNB dye is sensitive to Mg^{2+} concentration. So, Mg^{2+} has a dual role in this process. To balance the effect of Mg^{2+} concentration on both signal and enzyme activity, an experiment was designed in the constant concentration of target (0.4 pM), PLP (0.6 pM) and dNTP (2 mM) and different concentrations of $MgSO_4$ (4.0, 6.0 8.0, 10.0 and 12.0 mM) (Fig. 2C). Although increasing the concentration of Mg^{2+} enhances the bio-catalytic activity of DNA polymerase, it may interfere in the color transition of the HNB dye. Accordingly, the optimum concentration for Mg^{2+} was obtained as 8 mM (Inset 1). This also can be easily observed by naked-eyes (Inset 2).

3.4. Specificity

One of the most important aspects of a biosensor is its specificity toward particular target in a complex matrix. In order to meet the expectation of specificity, the responses of biosensor toward H_5N_1 target was compared to H_3N_8 (as an influenza A virus subtype which also infects the poultries) as a similar sample and two other targets including genomic DNA and hepatitis B virus (HBV). It is clear from the Fig. 3 that significant signal was achieved by H_5N_1 target, while the signals for the other targets were close to the negative control (blank). This also can be recognized even via naked-eye (Inset). Furthermore, the recognition sequence for PLP was checked by basic local alignment search tool (BLAST) program (http://blast.ncbi.nlm.nih.gov/Blast) and no nucleotide variation were detected in the PLP target sequence that have been reported in genomic database (http://www.ncbi.nlm.nih.gov). As a result, one may conclude that this biosensor has ability to detect all available H_5N_1 subtypes. It is also worth noticing that re-assortment of the influenza A viruses genomes may lead to emerge new influenza A subtypes through the mechanism of antigenic shift (Hamidi et al. 2015; Webster et al. 1992). The recognition target for the PLP is also found in H_5N_5 subtype, but it still has been reported one time in the genomic database and hence it cannot conclude the feasibility of the application of this biosensor for H_5N_5 subtype (Hamidi et al. 2015).

3.5. Calibration curve for H_5N_1

For colorimetric determination of target, the HNB absorbance (RCA signal) was recorded at optimized conditions in the presence of different concentrations of H_5N_1 (Fig. 4, Inset A). By increasing the target concentration the absorbance intensity at 650 nm was increased linearly and finally ascended to a plateau (Insets A and C). As seen, the linear range was limited to 0.16-0.80 pM

(Inset C). However, by plotting the absorbance signal against logarithm of target concentration a wider linear range (0.16 to 1.20 pM) was obtained. Based on the Eq. 1 (Hamidi et al. 2015) the detection limit (DL) at signal to noise ratio of 3 was estimated to be about 28 femtomolar (fM).

$$DL = 3.3\ \sigma/S \qquad (1)$$

Where, σ and S indicate standard deviation and slope of calibration curve, respectively. The calculated regression equation for H_5N_1 was I = 1.139 log [H5N1] – 1.324 (R2 = 0.98, n = 3), and the relative standard deviation for H_5N_1 biosensor at the concentration of 0.16 pM was 0.01%. It is important to note that the H_5N_1 containing samples are also visible even by naked-eye in the concentrations above ~ 0.40 pM of H_5N_1 (Inset B).

As shown in Table 1, comparing with the other systems reported in the literature (Niessen and Vogel 2010; Peng et al. 2014; Russell et al. 2014; Yang et al. 2007; Zhou et al. 2012), this biosensor has some advantages: i) Application of PLP which high specifically detects its target is followed by circularizing upon the action of ligase enzyme and leads to signal amplification via HRCA reaction (Larsson et al. 2004). ii) Replacement of heat shock by pH shock not only makes the experiment much easier but also preserves DNA from possible break down that occurs at high temperatures (Hamidi et al. 2015). iii) By applying the large fragment Bst DNA polymerase, the HRCA reaction is much improved and higher signal is obtained (Lizardi et al. 1998; Zhang et al. 2001a). iv) Furthermore in this system for the first time we coupled HNB dye with RCA reaction that makes easy to recognize the target. Thus, by using isothermal RCA reaction not only the need for thermal cycler instrument was excluded, but also the demand for expensive devices for qualitative detection was omitted. v) As compared with the other colorimetric dyes such as calcein with $MnCl_2$ and Quant-iT PicoGreen, HNB has been reported

to be the best, because it is an inexpensive, accurate and also easy to observe by naked-eye (Wastling et al. 2010). vi) Besides, the change in the color of HNB is stable (Goto et al. 2009) which remains intact for two months. All in all, this biosensor has potential to be used for commercial purposes due to being label free, easy to set up and its colorimetric nature.

3.6. Determination of H_5N_1 in real sample

In order to examine the feasibility of H_5N_1 biosensor for real samples, five H_5N_1 samples from infected birds were obtained from Tehran University of Medical Sciences and their concentration were determined by conventional real-time PCR as 0.32, 0.26, 0.20, 0.40 and 0.45 pM. Thereafter, the samples concentrations were determined by the biosensor. According to the calibration curve equation (Fig. 6), the mean values of concentrations of the samples were calculated to be 0.31 ± 0.008, 0.24 ± 0.005, 0.18 ± 0.003, 0.38 ± 0.007 and 0.42 ± 0.006 pM. By comparing the results of real-time PCR with those obtained by HRCA biosensor, a fine consistency was achieved. Thus, one may conclude that this biosensor has feasibility to detect H_5N_1 virus in real samples.

4. Conclusion

A simple and sensitive technique was developed for detection of H_5N_1 virus. A procedure for application of HNB as metal indicator for monitoring of RCA reaction via the changes in the concentration of soluble Mg^{2+} was established. Based on the type of application, the technique can be used either as a quantitative biosensor using UV-Vis spectroscopy or a qualitative system using naked eye. HRCA reaction based on PLP and Bst DNA polymerase led to signal amplification so that an excellent DL (28 fM) was obtained. Furthermore, replacement of the heat shock with pH shock also increased the efficiency of the reaction via the inhibition of the

possible DNA breaks. Moreover, feasibility of the determination of real H_5N_1 samples confirms the practical aspect of this biosensor in real conditions. As a result, it seems that this biosensor could be applicable for commercial purposes due to the simplicity of isothermal DNA amplification technique and colorimetric method used in this assay.

References

Banér, J., Nilsson, M., Mendel-Hartvig, M., Landegren, U., 1998. Nucleic Acids Res. 26, 5073-5078.

Brittain, H.G., 1977. Anal. chem. 49, 969-972.

Dawson, E.D., Moore, C.L., Dankbar, D.M., Mehlmann, M., Townsend, M.B., Smagala, J.A., Smith, C.B., Cox, N.J., Kuchta, R.D., Rowlen, K.L., 2007. Anal. chem. 79, 378-384.

Demidov, V.V., 2002. Expert Rev. Mol. Diagn. 2, 542-548.

Goto, M., Honda, E., Ogura, A., Nomoto, A., Hanaki, K.I., 2009. Biotechniques 46, 167-172.

Gyarmati, P., Conze, T., Zohari, S., LeBlanc, N., Nilsson, M., Landegren, U., Banér, J., Belák, S., 2008. J. Clin. Microbiol. 46, 1747-1751.

Hamidi, S.V., Ghourchian, H., Tavoosidana, G., 2015. Analyst 140, 1502-1509.

Ito, A., Ueno, K., 1970. Jpn. Analyst 19, 393-397.

Kaocharoen, S., Wang, B., Tsui, K.M., Trilles, L., Kong, F., Meyer, W., 2008. Electrophoresis 29, 3183-3191.

Larsson, C., Koch, J., Nygren, A., Janssen, G., Raap, A.K., Landegren, U., Nilsson, M., 2004. Nat. Methods 1, 227-232.

Li, K., Guan, Y., Wang, J., Smith, G., Xu, K., Duan, L., Rahardjo, A., Puthavathana, P., Buranathai, C., Nguyen, T., 2004. Nature 430, 209-213.

Liang, K., Zhai, S., Zhang, Z., Fu, X., Shao, J., Lin, Z., Qiu, B., Chen, G.N., 2014. Analyst 139, 4330-4334.

Lizardi, P.M., Huang, X., Zhu, Z., Bray-Ward, P., Thomas, D.C., Ward, D.C., 1998. Nat. Genet. 19, 225-232.

Ma, X.J., Shu, Y.L., Nie, K., Qin, M., Wang, D.Y., Gao, R.B., Wang, M., Wen, L.Y., Han, F., Zhou, S. M., 2010. J. Virol. Methods 167, 214-217.

Molinari, N.A.M., Ortega-Sanchez, I.R., Messonnier, M.L., Thompson, W.W., Wortley, P.M., Weintraub, E., Bridges, C.B., 2007. Vaccine 25, 5086-5096.

Mori, Y., Kitao, M., Tomita, N., Notomi, T., 2004. J. Biochem. Biophys. Methods 59, 145-157.

Mori, Y., Nagamine, K., Tomita, N., Notomi, T., 2001. Biochem. Biophys. Res. Commun. 289, 150-154.

Nahar, S., Ahmed, M.U., Safavieh, M., Rochette, A., Toro, C., Zourob, M., 2015. Analyst 140, 931-937.

Nakajima, J., Mizogami, K., Ukena, Y., 2003. U.S. Patent No. 6,599,748.

Nie, K., Zhao, X., Ding, X., Li, X., Zou, S., Guo, J., Wang, D., Gao, R., Li, X., Huang, W., 2013. Clin. Microbiol. Infec. 19, e372-e375.

Niessen, L., Vogel, R.F., 2010. Int. J. Food Microbiol. 140, 183-191.

Nijhuis, M., van Maarseveen, N., Schuurman, R., Verkuijlen, S., de Vos, M., Hendriksen, K., van Loon, A.M., 2002. J. Clin. Microbiol. 40, 3666-3670.

Nilsson, M., Malmgren, H., Samiotaki, M., Kwiatkowski, M., Chowdhary, B.P., Landegren, U., 1994. Science 265, 2085-2088.

Peng, Y., Li, L., Yi, X., Guo, L., 2014. Biosens. Bioelectron. 59, 314-320.

Quan, P.L., Palacios, G., Jabado, O.J., Conlan, S., Hirschberg, D.L., Pozo, F., Jack, P.J., Cisterna, D., Renwick, N., Hui, J., 2007. J. Clin. Microbiol. 45, 2359-2364.

Rector, A., Tachezy, R., Van Ranst, M., 2004. J. Virol. 78, 4993-4998.

Russell, C., Welch, K., Jarvius, J., Cai, Y., Brucas, R., Nikolajeff, F., Svedlindh, P., Nilsson, M., 2014. ACS nano 8, 1147-1153.

Safavieh, M., Ahmed, M.U., Sokullu, E., Ng, A., Braescu, L., Zourob, M., 2014. Analyst 139, 482-487.

Steain, M.C., Dwyer, D.E., Hurt, A.C., Kol, C., Saksena, N.K., Cunningham, A.L., Wang, B., 2009. Antiviral Res. 84, 242-248.

Steitz, T.A., 1998. Nature 391, 231-232.

Stöhr, K., 2003. Vaccine 21, 1744-1748.

Thai, H.T.C., Le, M.Q., Vuong, C.D., Parida, M., Minekawa, H., Notomi, T., Hasebe, F., Morita, K., 2004. J. Clin. Microbiol. 42, 1956-1961.

Tomita, N., Mori, Y., Kanda, H., Notomi, T., 2008. Nat. Protoc. 3, 877-882.

Wang, B., Potter, S.J., Lin, Y., Cunningham, A.L., Dwyer, D.E., Su, Y., Ma, X., Hou, Y., Saksena, N.K., 2005. J. Clin. Microbiol. 43, 2339-2344.

Wang, D., Coscoy, L., Zylberberg, M., Avila, P.C., Boushey, H.A., Ganem, D., DeRisi, J.L., 2002. PNAS 99, 15687-15692.

Wang, P., Zhang, T., Yang, T., Jin, N., Zhao, Y., Fan, A., 2014. Analyst 139, 3796-3803.

Wastling, S.L., Picozzi, K., Kakembo, A.S., Welburn, S.C., 2010. PLoS Negl. Trop. Dis. 4, e865.

Webster, R.G., Bean, W.J., Gorman, O.T., Chambers, T.M., Kawaoka, Y., 1992. Microbiol. Rev. 56, 152-179.

Williams, B.G., Gouws, E., Boschi-Pinto, C., Bryce, J., Dye, C., 2002. Lancet Infect. Dis. 2, 25-32.

Yang, L., Fung, C.W., Cho, E.J., Ellington, A.D., 2007. Anal. Chem. 79, 3320-3329.

Yoneyama, T., Kiyohara, T., Shimasaki, N., Kobayashi, G., Ota, Y., Notomi, T., Totsuka, A., Wakita, T., 2007. J. Virol. Methods 145, 162-168.

Zhang, D.Y., Brandwein, M., Hsuih, T., Li, H.B., 2001a. Mol. Diagn. 6, 141-150.

Zhang, D.Y., Zhang, W., Li, X., Konomi, Y., 2001b. Gene 274, 209-216.

Zhang, J., Feng, Y., Hu, D., L., H., Zhu, J., Cao, M., Zheng, F., Zhu, J., Gong, X., Hao, L., 2013. J. Clin. Microbiol. 51, 3760-3764.

Zhou, X., Su, Q., Xing, D., 2012. Anal. Chim. Acta 713, 45-49.

Figures captions

Scheme 1: Illustration of the HRCA technique for colorimetric determination of H_5N_1. I: In this step at first denaturation solution (pH~12) was added to the PLP and H_5N_1 mixture and then the neutralizing solution was gradually injected to hybridize PLP with H_5N_1. II: In order to seal the PLP head to tail and make a circular probe, the mixture was treated with T_4 ligase enzyme for 60 min at 37 ºC. III: Exonuclease enzyme degrades H_5N_1 from the direction of 3′ to 5′ for 30 min at 37 ºC. This free 3′ end, then is used as a primer for Bst polymerase for initiation of the RCA reaction. IV: The circular PLPs are then served as template for HRCA reaction in the presence of HNB dye. This leads to form the high molecular weight dsDNA. While the reaction is progressed the produced PPi^- molecules are chelated with Mg^{2+} ions that cause increment in the intensity of HNB absorbance in 650 nm. This process can be detected by measurement of absorbance intensity after incubation in 63 ºC for 60 min or simply can be visualized by naked eyes.

Fig. 1: Agarose gel electrophoresis of HRCA product. Lane M: markers (nt standards for nucleotide). Lane A: blank (without H_5N_1 targets). Lanes B: HRCA products. The electrophoresis was performed using 1% agarose gel (20 cm length) for 30 min. The applied voltage was 90 V.

Fig. 2: Optimization of analytical parameters of HRCA reaction. A) The PLP concentration was optimized in the presence of constant concentration of target (0.40 pM) and different concentrations of PLP (from down to up: 0, 0.2, 0.4, 0.6 and 0.8 pM). Inset 1 indicates the absorbance changes at 650 nm. Inset 2, shows the color change due to the increment of PLP concentration. B) The dNTP concentration was optimized in the presence of constant

concentration of target (0.40 pM), PLP (0.60) and different concentrations of dNTP (from down to up: 0, 0.50, 1.0, 1.50, 2.0 and 2.50 mM). Inset 1, indicates the absorbance changes at 650 nm. Inset 2, indicates the color change due to the increment of dNTP concentration. C) The $MgSO_4$ concentration was optimized in the presence of constant concentration of target (0.40 pM), PLP (0.60 pM), dNTP (2 mM) and different concentrations of $MgSO_4$ (from down to up: 12.0, 10.0, 4.0, 6.0 and 8.0 mM). Inset 1, indicates the absorbance changes at 650 nm. Inset 2, illustrates the color change due to the increment of $MgSO_4$ concentration .The arrows in the pictures show the direction for increasing concentration. The HRCA reaction was carried out at 63 °C.

Fig. 3: Comparison of specificity of H_5N_1 biosensor towards different DNA samples. HRCA signal was recorded toward different molecules of H_5N_1, genomic DNA, HBV, H_3N_8 and blank as negative control. In all measurements the concentration of samples was 0.8 pM. The experiments were carried out at 63 °C and PLP concentration of 0.6 pM. The image in the inset shows the color change due to the presence of H_5N_1, genomic DNA, HBV, H_3N_8 and blank as negative control from left to right, respectively.

Fig. 4: Calibration curve for colorimetric determination of H5N1. Inset A shows the absorbance of RCA signal recorded at different concentrations of H5N1 (from down to up: 0, 0.04, 0.16, 0.24, 0.32, 0.36, 0.50, 0.60, 0.80, 1.20 and 1.60 pM) at 63 °C. Inset B illustrates the images of color change due to the increment of H5N1 concentration. (The arrow shows the direction for increasing concentration). Inset C shows the HNB absorbance changes against H5N1 concentration.

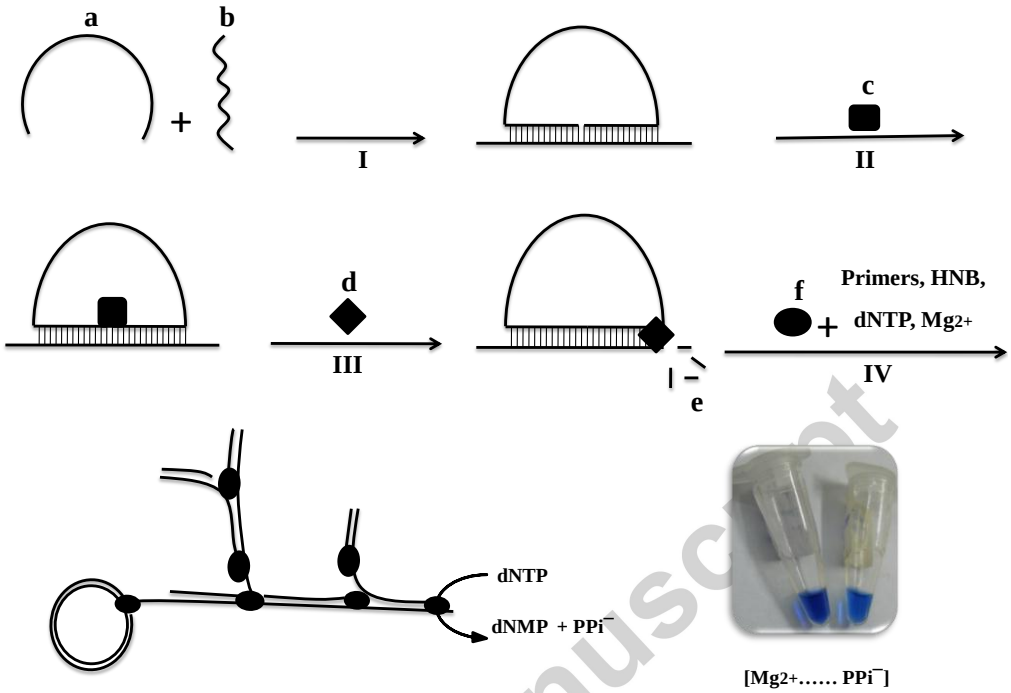

a: Linear PLP (L-PLP) **d: Exonuclease enzyme** **e: Nucleotides**

b: H_5N_1 target **f: Large fragment of Bst DNA polymerase**

c: T_4 DNA ligase enzyme **dNMP: Deoxyribonucleotide monophosphate**

Scheme 1

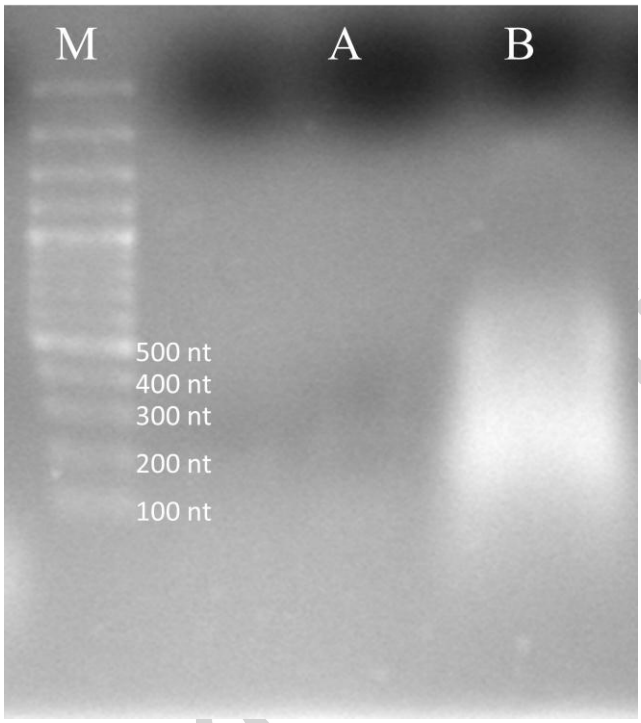

Fig. 1

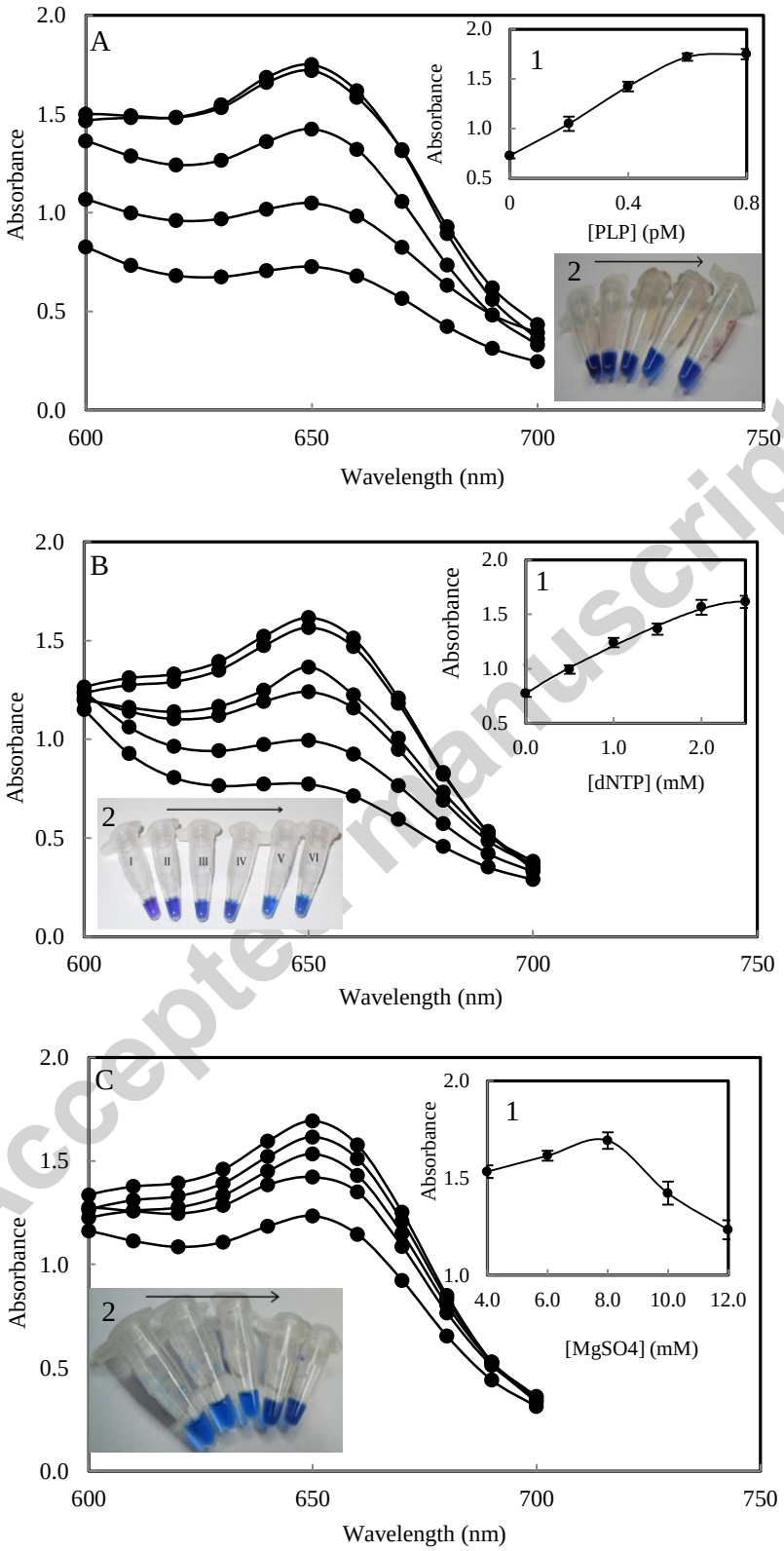

Fig. 2

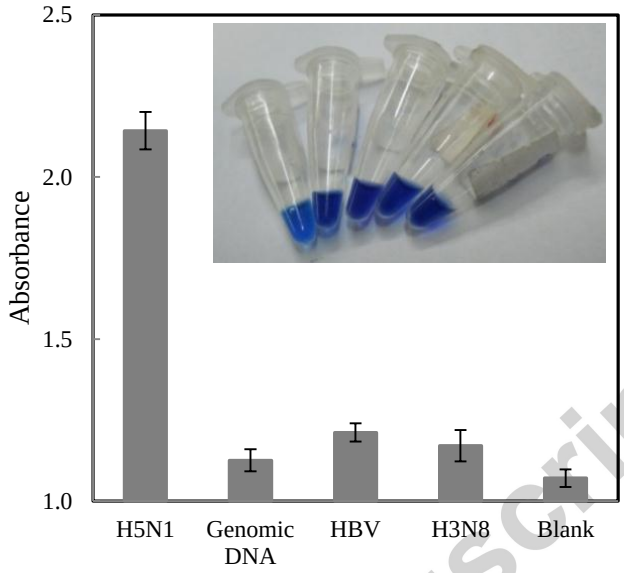

Fig. 3

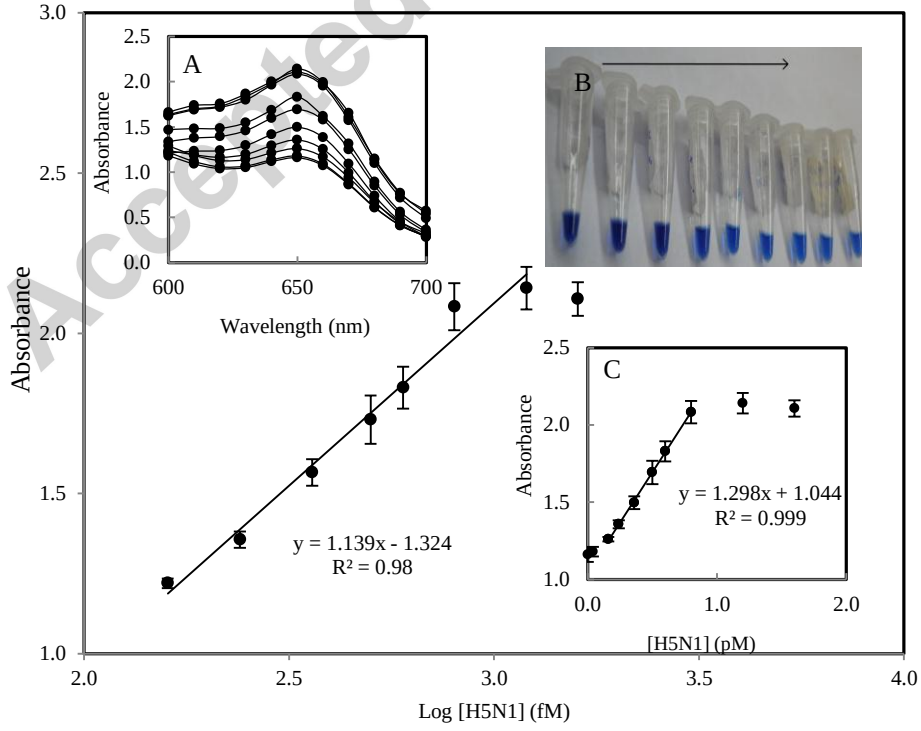

Fig. 4

Table 1 Comparison between different parameters obtained by the present biosensor with those reported in literatures.

Target	Method	Detection method	Linear range	Label free	Number of primers	Detection limit (pM)	References
H_5N_1 virus	RCA	Colorimetric (HNB)	0.16 -1.20 (pM)	+	2	0.028	Present work
Fusarium graminearum	LAMP	Colorimetric (Calcein)	---	+	6	0.85	(Niessen and Vogel 2010)
Pb^{2+}	RCA	Electrochemical	1 (pM) -1 (μM)	+	1	0.29	(Peng et al. 2014)
PDGF†	RCA	Fluorescence	0.4-80 (nM)	+	2	400	(Yang et al. 2007)
Hg^{2+}	RCA	Electrochemiluminescent	0.1-1000 (nM)	-	1	100	(Zhou et al. 2012)
Escherichia coli	RCA	Electrical	0.1-10 (pM)	-	1	0.10	(Russell et al. 2014)

† Platelet-derived growth factor

Highlights

A procedure for application of hydroxy naphthol blue as metal indicator for monitoring of hyperbranched rolling circle amplification reaction (HRCA) via the changes in the concentration of soluble Mg^{2+} was established.

Based on the types of applications the system can be used either as a quantitative biosensor using UV-Vis spectroscopy or a qualitative system using naked eye.

HRCA reaction based on padlock probe and Bst DNA polymerase led to signal amplification so that an excellent deyection limit (25 fM) was obtained.

Replacement of the heat shock with pH shock also increased the efficiency of the reaction via the inhibition of the possible DNA breaks.

The biosensor could be applicable for commercial purposes due to the simplicity of isothermal DNA amplification technique and colorimetric method used in this assay.